Long-Term Satellite Record Reveals Likely Recent Aerosol Trend

Michael I. Mishchenko,* Igor V. Geogdzhayev, William B. Rossow, Brian Cairns, Barbara E. Carlson, Andrew A. Lacis, Li Liu, Larry D. Travis

Recent observations of downward solar radiation fluxes at Earth's surface have shown a recovery from the previous decline known as global "dimming" (*1*), with the "brightening" beginning around 1990 (*2*). The increasing amount of sunlight at the surface profoundly affects climate and may represent certain diminished counterbalances to greenhouse gas warming, thereby making the warming trend more evident during the past decade.

It has been suggested that tropospheric aerosols have contributed notably to the switch from solar dimming to brightening via both direct and indirect aerosol effects (*1*, *2*). It has further been argued (*3*) that the solar radiation trend mirrors the estimated recent trend in primary anthropogenic emissions of SO_2 and black carbon, which contribute substantially to the global aerosol optical thickness (AOT). A similar increase of net solar flux at the top of the atmosphere (TOA) over the same period appears to be explained by corresponding changes in lower-latitude cloudiness (*4*), which confounds the interpretation of the surface radiation record. Therefore, it is important to provide a direct and independent assessment of the actual global long-term behavior of the AOT. We accomplish this by using the longest uninterrupted record of global satellite estimates of the column AOT over the oceans, the Global Aerosol Climatology Project (GACP) record (*5*). The record is derived from the International Satellite Cloud Climatology Project (ISCCP) DX radiance data set composed of calibrated and sampled Advanced Very High Resolution Radiometer (AVHRR) radiances. A detailed discussion of the sampling resolution, calibration history, and changes in the corresponding satellite sensors can be found in (*6*).

The global monthly average of the column AOT is depicted for the period August 1981 to June 2005 (Fig. 1, solid black curve). The two major maxima are caused by the stratospheric aerosols generated by the El Chichon (March 1982) and the Mount Pinatubo (June 1991) eruptions, also captured in the Stratospheric Aerosol and Gas Experiment (SAGE) stratospheric AOT record (*7*). The quasi-periodic oscillations in the black curve are the result of short-term aerosol variability.

The overall behavior of the column AOT during the eruption-free period from January 1986 to June 1991 (Fig. 1, red line) shows only a hint of a statistically significant tendency and indicates that the average column AOT value just before the Mount Pinatubo eruption was close to 0.142. After the eruption, the GACP curve is a superposition of the complex volcanic and tropospheric AOT temporal variations. However, the green line reveals a long-term decreasing tendency in the tropospheric AOT. Indeed, even if we assume that the stratospheric AOT just before the eruption was as large as 0.007 and that by June 2005 the stratospheric AOT became essentially zero (compare with the blue curve), still the resulting decrease in the tropospheric AOT during the 14-year period comes out to be 0.03. This trend is significant at the 99% confidence level.

Admittedly, AVHRR is not an instrument designed for accurate aerosol retrievals from space. Among the remaining uncertainties is radiance calibration, which, if inaccurate, can result in spurious aerosol tendencies. Similarly, substantial systematic changes in the aerosol single-scattering albedo or the ocean reflectance can be misinterpreted in terms of AOT variations. However, the successful validation of GACP retrievals using precise sun photometer data taken from 1983 through 2004 (*8*, *9*) indicates that the ISCCP radiance calibration is likely to be reliable. This conclusion is reinforced by the close correspondence of calculated and observed TOA solar fluxes (*4*). Furthermore, the GACP AOT record appears to be self-consistent, with no drastic intrasatellite variations, and is consistent with the SAGE record.

The advantage of the AVHRR data set over the data sets collected with more advanced recent satellite instruments is its duration, which makes possible reliable detection of statistically significant tendencies like the substantial decrease of the tropospheric AOT between 1991 and 2005. With all the uncertainties, the tropospheric AOT decrease over the 14-year period is estimated to be at least 0.02. This change is consistent with long-term atmospheric transmission records collected in the former Soviet Union (*5*).

Our results suggest that the recent downward trend in the tropospheric AOT may have contributed to the concurrent upward trend in surface solar fluxes. Neither AVHRR nor other existing satellite instruments can be used to determine unequivocally whether the recent AOT trend is due to long-term global changes in natural or anthropogenic aerosols. This discrimination would be facilitated by an instrument like the Aerosol Polarimetry Sensor (APS), scheduled for launch in December 2008 as part of the NASA Glory mission (*10*). It is thus imperative to provide uninterrupted multidecadal monitoring of aerosols from space with dedicated instruments like APS in order to detect long-term anthropogenic trends potentially having a strong impact on climate.

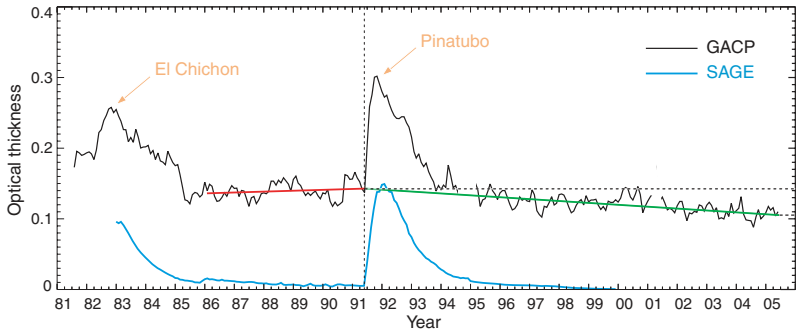

Fig. 1. GACP record of the globally averaged column AOT over the oceans and SAGE record of the globally averaged stratospheric AOT.

References and Notes

1. M. Wild *et al.*, *Science* **308**, 847 (2005).
2. R. T. Pinker, B. Zhang, E. G. Dutton, *Science* **308**, 850 (2005).
3. D. G. Streets, Y. Wu, M. Chin, *Geophys. Res. Lett.* **33**, L15806 (2006).
4. Y. Zhang, W. B. Rossow, A. A. Lacis, V. Oinas, M. I. Mishchenko, *J. Geophys. Res.* **109**, D19105 (2004).
5. I. V. Geogdzhayev, M. I. Mishchenko, E. I. Terez, G. A. Terez, G. K. Gushchin, *J. Geophys. Res*. **110**, D23205 (2005); and references therein.
6. W. B. Rossow, R. A. Schiffer, *Bull. Am. Meteorol. Soc.* **80**, 2261 (1999); and references therein.
7. J. Hansen *et al.*, *J. Geophys. Res.* **107**, 4347 (2002).
8. L. Liu *et al.*, *J. Quant. Spectrosc. Radiat. Transfer* **88**, 97 (2004).
9. A. Smirnov *et al.*, *Geophys. Res. Lett.* **33**, L14817 (2006).
10. M. I. Mishchenko *et al.*, *J. Quant. Spectrosc. Radiat. Transfer* **88**, 149 (2004).
11. This research is part of NASA/Global Energy and Water Cycle Experiment GACP and was funded by the NASA Radiation Sciences Program, managed by H. Maring and D. Anderson.

24 October 2006; accepted 20 December 2006
10.1126/science.1136709

NASA Goddard Institute for Space Studies, 2880 Broadway, New York, NY 10025, USA.

*To whom correspondence should be addressed. E-mail: mmishchenko@giss.nasa.gov

REVIEW

Perspectives on the Arctic's Shrinking Sea-Ice Cover

Mark C. Serreze,[1]* Marika M. Holland,[2] Julienne Stroeve[1]

Linear trends in arctic sea-ice extent over the period 1979 to 2006 are negative in every month. This ice loss is best viewed as a combination of strong natural variability in the coupled ice-ocean-atmosphere system and a growing radiative forcing associated with rising concentrations of atmospheric greenhouse gases, the latter supported by evidence of qualitative consistency between observed trends and those simulated by climate models over the same period. Although the large scatter between individual model simulations leads to much uncertainty as to when a seasonally ice-free Arctic Ocean might be realized, this transition to a new arctic state may be rapid once the ice thins to a more vulnerable state. Loss of the ice cover is expected to affect the Arctic's freshwater system and surface energy budget and could be manifested in middle latitudes as altered patterns of atmospheric circulation and precipitation.

The most defining feature of the Arctic Ocean is its floating sea-ice cover, which has traditionally ranged from a maximum extent of about 16×10^6 km^2 in March to a minimum extent of 7×10^6 km^2 at the end of the summer melt season in September (Fig. 1). Consistent satellite-derived monthly time series of sea-ice extent are provided by the Nimbus-7 Scanning Multichannel Microwave Radiometer (October 1978 to August 1987) and the Defense Meteorological Satellite Program Special Sensor Microwave/Imager (1987 to present). Based on regression analysis of the combined record over the period 1979 to 2006, ice extent has declined for every month (Fig. 2), most rapidly for September, for which the trend is –8.6 ± 2.9% per decade or about 100,000 km^2 per year. Ice extent is defined as the area of the ocean with a fractional ice cover (i.e., an ice concentration) of at least 15% (*1*–*3*).

Every year since 2001 has yielded pronounced September minima, the most extreme of which was in 2005 (5.56×10^6 km^2). When compared to the mean ice extent over the period 1979 to 2000, this represents a spatial reduction of 21% (1.6×10^6 km^2), an area roughly the size of Alaska (Fig. 1). Comparisons with earlier records, which combine visible-band satellite imagery and aircraft and ship reports, suggest that the September 2005 ice extent was the lowest in at least the past 50 years. Data for the past few years suggest an accelerating decline in winter sea-ice extent (*4*).

Fig. 1. Sea-ice extent (bright white area) for September 2005. Median ice extents based on the period 1979 to 2000 for September (red line) and March (blue line) illustrate the typical seasonal range. Geographic features referred to in the text are labeled. Credit: NSIDC image in Google Earth.

Evidence for accompanying reductions in ice thickness (*5*) is inconclusive. Upward-looking sonar aboard submarines provides information on ice draft—the component of the total thickness (about 90%) that projects below the water surface. Comparisons between early sonar records (1958 to 1976) and those for 1993 to 1997 indicate reductions of 1.3 m in mean late summer ice draft over much of the central Arctic Ocean (*6*), but sparse sampling complicates interpretation. Further analysis of the submarine-acquired data in conjunction with model simulations points to thinning through 1996 but modest recovery thereafter (*7*). Results from an ice-tracking algorithm applied to satellite data from 1978 to 2003 document decreasing coverage of old, thick ice (*8*).

Understanding the Observed Ice Loss

The observed decline in ice extent reflects a conflation of thermodynamic and dynamic processes. Thermodynamic processes involve changes in surface air temperature (SAT), radiative fluxes, and ocean conditions. Dynamic processes involve changes in ice circulation in response to winds and ocean currents. These include changes in the strength and location of the Beaufort Gyre (a mean annual clockwise motion in the western Arctic Ocean) and characteristics of the Transpolar Drift Stream (a motion of ice that progresses from the coast of Siberia, across the pole, and into the North Atlantic via the Fram Strait). Nearly all of the ice export from the Arctic to the Atlantic occurs through this narrow strait between northern Greenland and Svalbard (Fig. 1).

Estimated rates of SAT change over the Arctic Ocean for the past several decades vary depending on the time period and season, as well as the data source being considered. Although natural variability plays a large role in SAT variations, the overall pattern is one of recent warming, which is in turn part of a global signal (*9*). Using a record that combined coastal station observations with data from drifting buoys (from 1979 onward) and Russian "North Pole" stations (1950 to 1991), Rigor *et al.* (*10*) found positive SAT trends from 1979 to 1997 that were most pronounced and widespread during spring. Although there are biases in the buoy data relative to the North Pole data, especially for October through April (*11*), independent evidence for warming during spring, summer, and autumn since 1981 is documented in clear-sky surface temperatures retrieved from advanced very-high-resolution radiometer satellite imagery (*12*). Further support for warming comes from analysis of satellite-derived passive microwave brightness temperatures that indicate earlier onset of spring melt and lengthening of the melt season (*13*), as well as from data from the Television Infrared Observation Satellites Operational Vertical Sounder that point to increased downwelling radiation to the surface in spring over the past decade, which is linked to increased cloud cover and water vapor (*14*). Our assessments of autumn and winter data fields from the National Centers for

[1]Cooperative Institute for Research in Environmental Sciences, National Snow and Ice Data Center, Campus Box 449, University of Colorado, Boulder, CO 80309–0449, USA. [2]National Center for Atmospheric Research, Post Office Box 3000, Boulder, CO 80307, USA.

*To whom correspondence should be addressed. E-mail: serreze@kryos.colorado.edu

Environmental Prediction and National Center for Atmospheric Research (NCEP-NCAR) reanalysis (*15*) point to strong surface and low-level warming for the period 2000 to 2006 relative to 1979 to 1999. Weaker warming is evident for summer.

All of these results are consistent with a declining ice cover. However, at least part of the recent cold-season warming seen in the NCEP-NCAR data is itself driven by the loss of ice, because this loss allows for stronger heat fluxes from the ocean to the atmosphere. The warmer atmosphere will then promote a stronger longwave flux to the surface.

Links have also been established between ice loss and changes in ice circulation associated with the behavior of the North Atlantic Oscillation (NAO), Northern Annular Mode (NAM), and other atmospheric patterns. The NAO refers to covariability between the strength of the Icelandic Low and that of the Azores High, which are the two centers of action in the North Atlantic atmospheric circulation. When both are strong (or weak), the NAO is in its positive (or negative) phase. The NAM refers to an oscillation of atmospheric mass between the Arctic and middle latitudes and is positive when arctic pressures are low and midlatitude pressures are high. The NAO and NAM are closely related and can be largely viewed as expressions of the same phenomenon.

From about 1970 through the mid-1990s, winter indices of the NAO-NAM shifted from negative to strongly positive. Rigor *et al.* (*16*) showed that altered surface winds resulted in a more cyclonic motion of ice and an enhanced transport of ice away from the Siberian and Alaskan coasts (i.e., a more pronounced Transpolar Drift Stream). This change in circulation fostered openings in the ice cover. Although these openings quickly refroze in response to low winter SATs, coastal areas in spring were nevertheless left with an anomalous coverage of young, thin ice. This thin ice then melted out in summer, which was expressed as large reductions in ice extent. Summer ice loss was further enhanced as the thinner ice promoted stronger heat fluxes to the atmosphere, fostering higher spring air temperatures and earlier melt onset.

Given that the NAO-NAM has regressed back to a more neutral state since the late 1990s (*17*), these processes cannot readily explain the extreme September sea-ice minima of recent years. Rigor and Wallace (*18*) argued that recent extremes represent delayed impacts of the very strongly positive winter NAO-NAM state from about 1989 to 1995. As the NAO-NAM rose to this positive state, shifts in the wind field not only promoted the production of thinner spring ice in coastal areas but flushed much of the Arctic's store of thick ice into the North Atlantic through Fram Strait.

Rothrock and Zhang (*19*) modified this view. Using a coupled ice-ocean model, they argued that although wind forcing was the dominant driver of declining ice thickness and volume from the late 1980s through mid-1990s, the ice response to generally rising air temperatures was more steadily downward over the study period (1948 to 1999). In other words, without the NAO-NAM forcing, there would still have been a downward trend in ice extent, albeit smaller than that observed. Lindsay and Zhang (*20*) came to similar conclusions in their modeling study. Rising air temperature has reduced ice thickness, but changes in circulation also flushed some of the thicker ice out of the Arctic, leading to more open water in summer and stronger absorption of solar radiation in the upper (shallower depths of the) ocean. With more heat in the ocean, thinner ice grows in autumn and winter.

Recent years have experienced patterns of atmospheric circulation in spring and summer fa-

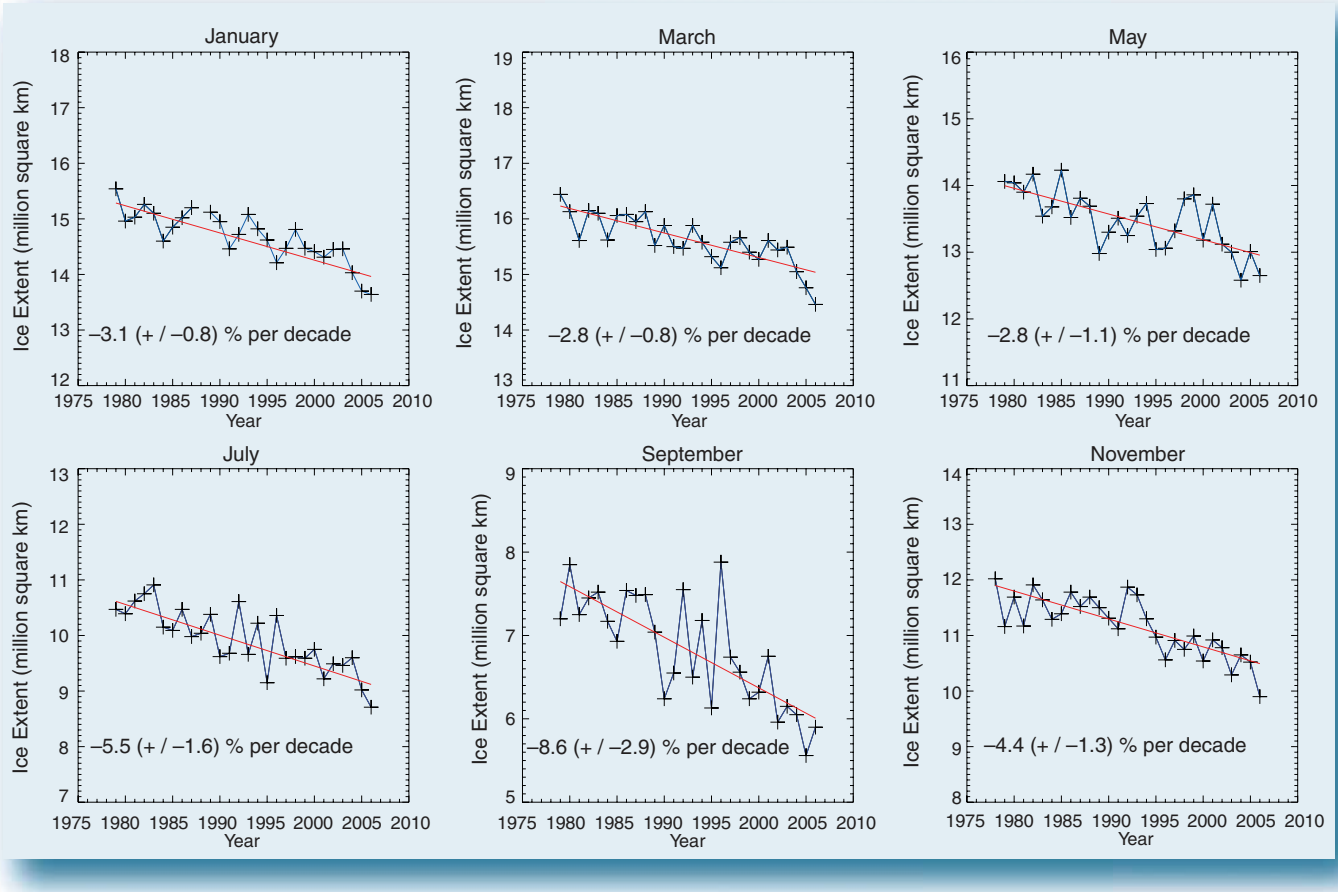

Fig. 2. Time series of arctic sea-ice extent for alternate months and least-squares linear fit based on satellite-derived passive microwave data from November 1979 through November 2006. Listed trends include (in parentheses) the 95% confidence interval of the slope. Ice extent is also declining for the six months that are not shown, ranging from –2.8 ± 0.8% per decade in February to –7.2 ± 2.3% per decade in August.

voring ice loss. By altering both the Beaufort Gyre and Transpolar Drift Stream, these patterns have reduced how long ice is sequestered and aged in the Arctic Ocean (*21*). The strength of a cyclonic atmospheric regime that sets up over the central Arctic Ocean in summer is important. Along with promoting offshore ice motion, the pronounced cyclonic summer circulations of 2002 and 2003 favored ice divergence, as is evident from the low ice concentrations in satellite imagery. Ice divergence in summer spreads the existing ice over a larger area, but enhanced absorption of solar energy in the areas of open water promotes stronger melt. There was also very little September ice in the Greenland Sea (off the east coast of Greenland) for these summers, which may also be linked to winds associated with this summer atmospheric pattern (*22*).

To further complicate the picture, it appears that changes in ocean heat transport have played a role. Warm Atlantic waters enter the Arctic Ocean through eastern Fram Strait and the Barents Sea and form an intermediate layer as they subduct below colder, fresher (less dense) arctic surface waters. Hydrographic data show increased import of Atlantic-derived waters in the early to mid-1990s and warming of this inflow (*23*). This trend has continued, characterized by pronounced pulses of warm inflow. Strong ocean warming in the Eurasian basin in 2004 can be traced to a pulse entering the Barents Sea in 1997 and 1998. The most recent data show another warm anomaly poised to enter the Arctic Ocean (*24*, *25*). These inflows may promote ice melt and discourage ice growth along the Atlantic ice margin. Once Atlantic water enters the Arctic Ocean, the cold halocline layer (CHL) separating the Atlantic and surface waters largely insulates the ice from the heat of the Atlantic layer. Observations suggest a retreat of the CHL in the Eurasian basin in the 1990s (*26*). This likely increased Atlantic layer heat loss and ice-ocean heat exchange. Partial recovery of the CHL has been observed since 1998 (*27*).

Maslowski *et al.* (*28*) proposed a connection between ice loss and oceanic heat flux through the Bering Strait. However, hydrographic data collected between 1990 and 2004 document strong variability in this inflow as opposed to a longer-term trend. An observed increase in the flux between 2001 and 2004 is estimated to be capable of melting 640,000 km^2 of 1-m-thick ice, but fluxes in 2001 are the lowest of the record (*29*). Subsequent analysis (*30*) nevertheless reveals a link between ice loss and increases in Pacific Surface Water (PSW) temperature in the Arctic Ocean beginning in the late 1990s, concurrent with the onset of sharp sea-ice reductions in the Chukchi and Beaufort seas. The hypothesis that has emerged from those observations is that delayed winter ice formation allows for more efficient coupling between the ocean and wind forcing. This redirects PSW from the shelf slope along Alaska into the Arctic Ocean, where it is more efficient in retarding winter ice growth. An imbalance between winter ice growth and summer melt results, accelerating ice loss over a large area.

To summarize, the observed sea-ice loss can in part be connected to arctic warming over the past several decades. Although this warming is part of a global signal suggesting a link with greenhouse gas (GHG) loading, attribution is complicated by a suite of contributing atmospheric and oceanic forcings. Below we review the evidence for an impact of GHG loading on the observed trends and projections for the future, based on climate model simulations.

Simulations from Climate Models

Zhang and Walsh (*31*) showed that most of the models used in the Intergovernmental Panel on Climate Change Fourth Assessment Report (IPCC AR4) have climatological sea-ice extent within 20% of the observed climatology over their adopted base period of 1979 to 1999, with good simulation of the seasonal cycle. The multimodel ensemble mean realistically estimates observed ice extent changes over this base period, and most individual models also show a downward trend. Our analysis of an IPCC AR4 multimodel ensemble mean hindcast for the longer base period 1979 to 2006 also reveals consistency with observations regarding larger trends in September versus those in winter. These results provide strong evidence that, despite prominent contributions of natural variability in the observed record, GHG loading has played a role.

Rates of ice loss both for the past few decades and those projected through the 21st century nevertheless vary widely between individual models. Our analyses show that in the IPCC AR4 models driven with the Special Report on Emissions Scenarios (SRES) A1B emissions scenario (in which atmospheric CO_2 reaches 720 parts per million by 2100), a near-complete or complete loss (to less than 1×10^6 km^2) of September ice will occur anywhere from 2040 to well beyond the year 2100, depending on the model and the particular run for that model. Overall, about half the models reach September ice-free conditions by 2100 (*32*). Figure 3 shows the spatial pattern of the percent of models that predict at least 15% fractional ice cover for March and September, averaging output over the period 2075–2084. Even by the late 21st century, most models project a thin ice cover in March. By contrast, about 40% of the models project no ice in September over the central Arctic Ocean.

The scatter among models reflects many factors, including the initial (late-20th century) simulated ice state, aspects of the modeled ocean circulation, simulated cloud conditions, and natural variability in the modeled system (e.g., NAO-NAM–like behavior). These tie in strongly to the strength and characteristics of the positive ice-albedo feedback mechanism. In general, GHG loading results in a stronger and longer summer melt season, thinning the ice and exposing more of the dark (low albedo) ocean surface that readily absorbs solar radiation. Autumn ice growth is delayed, resulting in thinner spring ice. This thin ice is more apt to melt out during the next summer, exposing more open water, which results in even thinner ice during the following spring. Negative feedbacks, such as the fact that thinner ice grows more rapidly than thicker ice when exposed to the same forcing, can counteract these changes but are generally weaker.

Although there is ample uncertainty regarding when a seasonally ice-free Arctic Ocean will be realized, the more interesting question is how it arrives at that state. Simulations based on the Community Climate System Model version 3 (CCSM3) (*33*) indicate that end-of-summer ice extent is sensitive to ice thickness in spring. If the ice thins to a more vulnerable state, a "kick" associated with natural climate variability can result in rapid summer ice loss because of the ice-albedo feedback. In

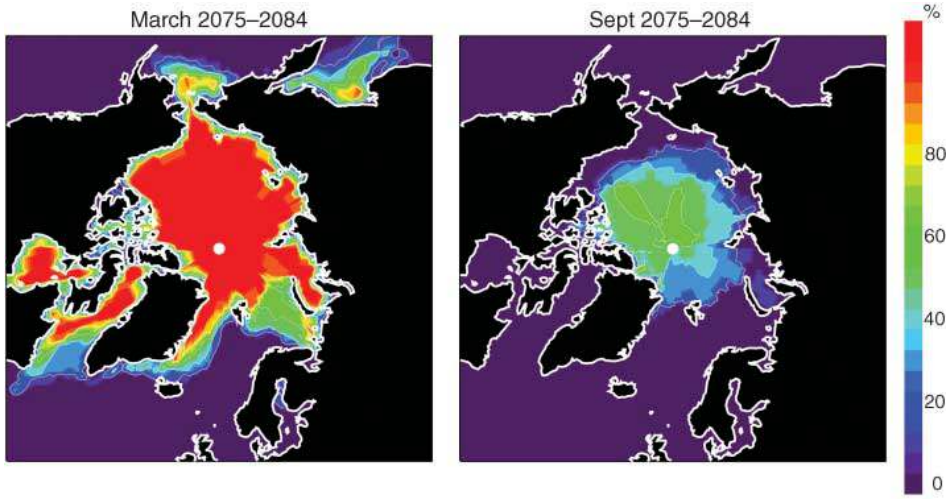

Fig. 3. Spatial pattern of the percent of IPCC AR4 model simulations (SRES A1B scenario) with at least 15% ice concentration for March (**left**) and September (**right**), averaged over the decade 2075 to 2084. For example, a value of 60% at a given location means that 60% of simulations predicted sea ice. Results are based on 11 models with realistic 20th-century September sea-ice extent.

the events simulated by CCSM3, anomalous ocean heat transport acts as this trigger. Such abrupt transitions are typically four times as fast as the observed trends over the satellite record. In one ensemble member, September ice extent decreases from about 6×10^6 to 2×10^6 km^2 in 10 years, resulting in near ice-free September conditions by 2040. A number of other climate models show similar rapid ice loss events.

Impacts

Loss of the sea-ice cover will have numerous impacts. A sharply warmer Arctic in autumn and winter is expected as a result of larger heat fluxes from the ocean to the atmosphere. This is the primary fingerprint of arctic amplification of greenhouse warming (*34*). As ice retreats from the shore, winds have a longer fetch over open water, resulting in more wave action. This effect is already resulting in coastal erosion in Alaska and Siberia. Ice loss is also affecting traditional hunting practices by members of indigenous cultures and contributing to regional declines in polar bear health and abundance (*35*).

In their modeling study, Magnusdottir *et al*. (*36*) found that declining ice in the Atlantic sector promotes a negative NAO-NAM atmospheric circulation response, with a weaker, southward-shifted storm track. Singarayer *et al*. (*37*) forced the Hadley Centre Atmospheric Model with observed sea ice from 1980 to 2000 and projected sea-ice reductions until 2100. In one simulation, mid-latitude storm tracks were intensified, increasing precipitation over western and southern Europe in winter. Experiments by Sewall and Sloan (*38*) revealed impacts on extrapolar precipitation patterns leading to reduced rainfall in the American West. Although results from different experiments with different designs vary, the common thread is that sea ice matters.

Climate models also indicate that by increasing upper-ocean stability and suppressing deepwater formation, North Atlantic freshening may disrupt the global thermohaline circulation, possibly with far-reaching consequences. Increased freshwater export from the Arctic is a potential source of such freshening. Observations implicate an arctic source for freshening in the North Atlantic since the 1960s (*39*). Total freshwater output to the North Atlantic is projected to increase through the 21st century, with decreases in ice export more than compensated by the liquid freshwater export. However, reductions in ice melt and associated freshening in the Greenland-Iceland-Norwegian (GIN) seas resulting from a smaller ice transport through Fram Strait may more directly affect the deepwater formation regions and counteract increased ocean stability due to the warming climate (i.e., a warmer upper ocean is more stable). This outcome could help maintain deepwater formation in the GIN seas (*40*).

Conclusions

Natural variability, such as that associated with the NAO-NAM and other circulation patterns, has and will continue to have strong impacts on the arctic sea-ice cover. However, the observed ice loss for the Arctic Ocean as a whole, including the larger trend for September as compared to that of winter, is qualitatively reproduced in ensemble mean climate model hindcasts forced with the observed rise in GHG concentrations. This strongly suggests a human influence (*31*). However, there is a large amount of scatter between individual simulations, which contributes to uncertainty regarding rates of ice loss through the 21st century. An emerging issue is how a seasonally ice-free Arctic Ocean may be realized: Will it result from a gradual decline with strong imprints of natural variability, or could the transition be rapid once the ice thins to a more vulnerable state? Links between altered ocean heat transport and observed ice loss remain to be resolved, as does the attribution of these transport changes, but pulses such as those currently poised to enter the Arctic Ocean from the Atlantic could provide a trigger for a rapid transition.

In this regard, future behavior of the CHL, which insulates the sea ice from the warm Atlantic layer, is a key wild card. Another uncertainty is the behavior of the NAO-NAM. Despite its return to a more neutral phase, there is evidence, albeit controversial, that external forcing may favor the positive state that promotes ice loss. The mechanisms are varied but in part revolve around the idea that stratospheric cooling in response to increasing GHG concentrations, or through ozone destruction, may "spin up" the polar stratospheric vortex, resulting in lower arctic surface pressures. Another view is that the NAO-NAM could be bumped to a preferred positive state via warming of the tropical oceans (*41*). However, as noted earlier, declining sea ice in the Atlantic sector may invoke a negative NAO-NAM response (*36*).

Given the agreement between models and observations, a transition to a seasonally ice-free Arctic Ocean as the system warms seems increasingly certain. The unresolved questions regard when this new arctic state will be realized, how rapid the transition will be, and what will be the impacts of this new state on the Arctic and the rest of the globe.

References and Notes

1. Ice extent time series are available from the National Snow and Ice Data Center (NSIDC) based on the application of the NASA team algorithm (used here) and a bootstrap algorithm to the passive microwave brightness temperatures (http:/nsidc.org/data/seaice/). Trends computed from both are negative in all months, but those from the bootstrap series are slightly smaller (which yielded a September trend of –7.9% per decade). Trends are computed from anomalies referenced to means over the period 1979 to 2000. Surface melt in summer contaminates the passive microwave signal, resulting in the underestimation of ice concentration. Use of ice extent (a binary ice–no ice classification) largely circumvents this problem.
2. Trends for all months are significant at the 99% confidence level, based on an *F* test with the null hypothesis of a zero trend. Trends are also significant (exceeding the 95% level) based on the approach of Weatherhead *et al.* (*3*), which computes the trend significance from the variance and autocorrelation of the residuals.

3. E. C. Weatherhead *et al.*, *J. Geophys. Res.* **103**, 10.1029/98JD00995 (1998).
4. J. C. Comiso, *Geophys. Res. Lett.* **33**, L18504 (2006).
5. Ice thickness can be described from a probability distribution, which has a peak at about 3 m. Although ice at the peak of the distribution is predominantly multiyear ice that has survived one or more melt seasons and thicker than younger first-year ice (representing a single year's growth), ridging can result in very thick first-year ice (up to 20 to 30 m).
6. D. A. Rothrock, Y. Yu, G. A. Maykut, *Geophys. Res. Lett.* **26**, 3469 (1999).
7. D. A. Rothrock, J. Zhang, Y. Yu, *J. Geophys. Res.* **108**, 3083 (2003).
8. C. Fowler, W. J. Emery, J. A. Maslanik, *IEEE Geosci. Remote Sens. Lett.* **1**, 71 (2004).
9. M. C. Serreze, J. A. Francis, *Clim. Change* **76**, 241 (2006).
10. I. G. Rigor, R. L. Colony, S. Martin, *J. Clim.* **13**, 896 (2000).
11. I. V. Polyakov *et al.*, *J. Clim.* **16**, 2067 (2003).
12. J. C. Comiso, *J. Clim.* **16**, 3498 (2003).
13. J. C. Stroeve, T. Markus, W. N. Meier, *Ann. Glaciol.* **25**, 382 (2006).
14. J. A. Francis, E. Hunter, *EOS Trans. Am. Geophys. Union* **87**, 509 (2006).
15. E. Kalnay *et al.*, *Bull. Am. Meteorol. Soc.* **77**, 437 (1996).
16. I. G. Rigor, J. M. Wallace, R. L. Colony, *J. Clim.* **15**, 2648 (2002).
17. J. E. Overland, M. Wang, *Geophys. Res. Lett.* **32**, L06701 (2005).
18. I. G. Rigor, J. M. Wallace, *Geophys. Res. Lett.* **31**, L09401 (2004).
19. D. A. Rothrock, J. Zhang, *J. Geophys. Res.* **110**, C01002 (2005).
20. R. W. Lindsay, J. Zhang, *J. Clim.* **18**, 4879 (2005).
21. J. A. Maslanik, S. Drobot, C. Fowler, W. Emery, R. Barry, *Geophys. Res. Lett.* **34**, 10.1029/2006GL028269 (2007).
22. J. C. Stroeve *et al.*, *Geophys. Res. Lett.* **32**, L04501 (2005).
23. R. R. Dickson *et al.*, *J. Clim.* **13**, 2671 (2000).
24. I. V. Polyakov *et al.*, *Geophys. Res. Lett.* **32**, L17605 (2005).
25. W. Walczowski, J. Piechura, *Geophys. Res. Lett.* **33**, L12601 (2006).
26. M. Steele, T. J. Boyd, *J. Geophys. Res.* **103**, 10419 (1998).
27. T. J. Boyd, M. Steele, R. D. Muench, J. T. Gunn, *Geophys. Res. Lett.* **29**, 1657 (2002).
28. W. Maslowski, D. C. Marble, W. Walczowski, A. J. Semtner, *Ann. Glaciol.* **33**, 545 (2001).
29. R. A. Woodgate, K. Aagaard, T. L. Weingartner, *Geophys. Res. Lett.* **33**, L15609 (2006).
30. K. Shimada *et al.*, *Geophys. Res. Lett.* **33**, L08605 (2006).
31. X. Zhang, J. E. Walsh, *J. Clim.* **19**, 1730 (2006).
32. O. Arzel, T. Fichefet, H. Goosse, *Ocean Model.* **12**, 401 (2006).
33. M. M. Holland, C. M. Bitz, B. Tremblay, *Geophys. Res. Lett.* **33**, L23503 (2006).
34. S. Manabe, R. J. Stouffer, *J. Geophys. Res.* **85**, 5529 (1980).
35. I. Stirling, C. L. Parkinson, *Arctic* **59**, 261 (2006).
36. G. Magnusdottir, C. Deser, R. Saravanan, *J. Clim.* **17**, 857 (2004).
37. J. S. Singarayer, J. Bamber, P. J. Valdes, *J. Clim.* **19**, 1109 (2006).
38. J. O. Sewall, L. C. Sloan, *Geophys. Res. Lett.* **31**, L06209 (2004).
39. B. J. Peterson *et al.*, *Science* **313**, 1061 (2006).
40. M. M. Holland, J. Finnis, M. C. Serreze, *J. Clim.* **19**, 6221 (2006).
41. N. P. Gillett, M. P. Baldwin, M. R. Allen, in *The North Atlantic Oscillation: Climate Significance and Environmental Impact*, J. W. Hurrell, Y. Kushnir, G. Ottersen, M. Visbeck, Eds. (American Geophysical Union, Washington, DC, 2003), Geophysical Monograph Series 134, chap. 9.

42. This study was supported by NSF, NASA, and NOAA. M. Savoie, L. Ballagh, W. Meier, and T. Scambos are thanked for their assistance.

10.1126/science.1139426

REVIEW

Recent Sea-Level Contributions of the Antarctic and Greenland Ice Sheets

Andrew Shepherd[1] and Duncan Wingham[2]*

After a century of polar exploration, the past decade of satellite measurements has painted an altogether new picture of how Earth's ice sheets are changing. As global temperatures have risen, so have rates of snowfall, ice melting, and glacier flow. Although the balance between these opposing processes has varied considerably on a regional scale, data show that Antarctica and Greenland are each losing mass overall. Our best estimate of their combined imbalance is about 125 gigatons per year of ice, enough to raise sea level by 0.35 millimeters per year. This is only a modest contribution to the present rate of sea-level rise of 3.0 millimeters per year. However, much of the loss from Antarctica and Greenland is the result of the flow of ice to the ocean from ice streams and glaciers, which has accelerated over the past decade. In both continents, there are suspected triggers for the accelerated ice discharge—surface and ocean warming, respectively—and, over the course of the 21st century, these processes could rapidly counteract the snowfall gains predicted by present coupled climate models.

Antarctica and Greenland hold enough ice to raise global sea levels by some 70 m (*1*) and, according to the geological record (*2*), collapses of Earth's former ice sheets have caused increases of up to 20 m in less than 500 years. Such a rise, were it to occur today, would have tremendous societal implications (*3*). Even a much more gradual rise would have great impact. Accordingly, one goal of glaciological survey [e.g., (*4*, *5*)] is to determine the contemporary sea-level contribution due to Antarctica and Greenland. For much of the 20th century, however, the size of these ice sheets hindered attempts to constrain their mass trends, because estimating whole–ice sheet mass change could be done only by combining sparse local surveys, with consequent uncertainty. For example, a 1992 review (*6*) concluded that the available glaciological measurements allowed Antarctica to be anything from a 600 Gt year^{-1} sink to a 500 Gt year^{-1} source of ocean mass [500 Gt of ice equals 1.4 mm equivalent sea level (ESL)], accounting for nearly all of the 20th-century sea-level trend of 1.8 mm year^{-1} (*1*) or, in the other direction, leaving a mass shortfall of some 1000 Gt year^{-1}. Even the 2001 Intergovernmental Panel on Climate Change (IPCC) report (*1*) preferred models to observations in estimating Antarctic and Greenland sea-level contributions.

However, in the past decade, our knowledge of the contemporary mass imbalances of Antarctica and Greenland has been transformed by the launch of a series of satellite-based sensors. Since 1998, there have been at least 14 satellite-based estimates (*7*–*20*) of the mass imbalance of Earth's ice sheets (Table 1). At face value, their range of some –366 to 53 Gt year^{-1}, or 1.0 to –0.15 mm year^{-1} sea-level rise equivalent, explains much of the eustatic component of 20th-century sea-level rise [1.5 mm year^{-1} in (*21*)], but we argue that the contribution is smaller and the problem of closing the 20th-century sea-level budget remains. Equally, the new observations provide a picture of considerable regional variability and, in particular, the long-predicted [e.g., (*1*)] snowfall-driven growth [e.g., (*10*, *22*)] is being offset by large mass losses from particular ice stream and glacier flows [e.g., (*12*, *23*)]. There is, moreover, evidence in Greenland and Antarctica of recent accelerations in these flows (*12*, *24*, *25*). It is apparent that the late 20th- and early 21st-century ice sheets at least are dominated by regional behaviors that are not captured in the models on which IPCC predictions have depended, and there is renewed speculation (*26*, *27*) of accelerated sea-level rise from the ice sheets under a constant rate of climate warming.

Although the observations in Table 1 have narrowed the uncertainty in estimates of the eustatic contribution to sea level, the range of values is notably wider than their stated uncertainties. Accordingly, we give consideration to the limitations of the three methods—accounting the mass budget [e.g., (*9*)], altimetry measurement of ice-sheet volume change [e.g., (*7*)], and observing the ice sheets' changing gravitational attraction [e.g., (*11*)]—used to calculate the estimates in Table 1. In light of these limitations, we discuss the recent changes in the Antarctic and Greenland ice sheets (AIS and GIS), and we conclude with some remarks on the future evolution of the ice sheets.

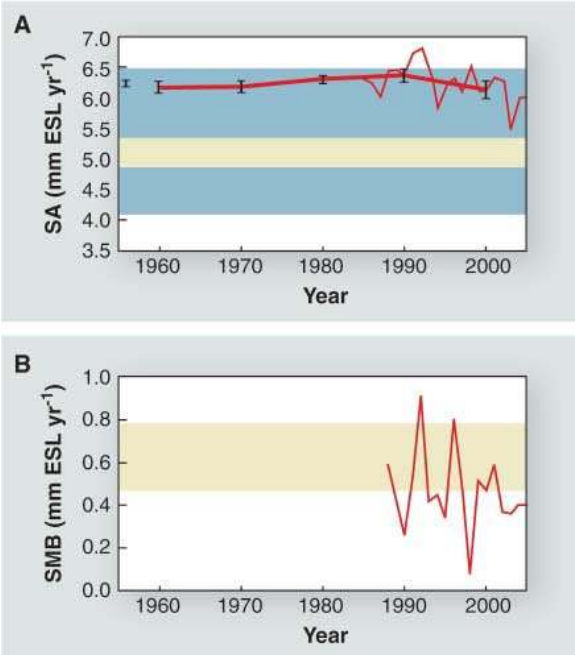

Fig. 1. Fluctuations in (**A**) the rate of snow accumulation (SA) of Antarctica [redrawn from (*38*)] and (**B**) the net surface mass balance (SMB) of Greenland [drawn from the data of (*32*)], determined from model reanalyses of meteorological observations expressed as ESL rise. Also shown are the ranges of published mean accumulation rates determined from glaciological observations (yellow) and climate models (blue).

Methods and Their Sensitivity to Accumulation Rate

The mass-budget method [e.g., (*9*, *12*)] compares the mass gain due to snowfall to mass losses due to sublimation, meltwater runoff, and ice that flows into the ocean. It has been given new impetus by the capability of interferometric synthetic aperture radar (InSAR) to determine ice surface velocity. This has improved earlier estimates of the ice flux to the ocean (*5*) and provides a capability to identify accelerations of ice flow. The method is hampered by a lack of accurate accumulation and ice thickness data. For Antarctica, where surface melting is negligible, accumulation may be determined by spatially averaging the history of accumulation recorded in ice cores, or from meteorological forecast models. Estimates of the temporally averaged accumulation or "mean" accumulation range, respectively, from 1752 to 1924 Gt year^{-1} (*1*) and from 1475 to 2331 Gt year^{-1} (*28*). The meteorological data are acknowledged to be of inferior accuracy (*28*), and their wide range can perhaps be discounted. The range of the core-based estimates, which use substantially the same core records, arises from differences in their spatial interpolation. Recent compilations have used the satellite-observed microwave temperature, which is correlated with accumulation, to guide the interpolation, and a careful study (*29*) placed the

[1]Centre for Polar Observation and Modelling, School of Geosciences, University of Edinburgh, EH8 9XP, UK. [2]Centre for Polar Observation and Modelling, Department of Earth Sciences, University College London, WC1E 6BT, UK.

*To whom correspondence should be addressed. E-mail: Andrew.Shepherd@edu.ac.uk (A.S.); djw@cpom.ucl.ac.uk (D.W.)

error of individual drainage-basin accumulation at 5%. The extent to which this error may average out over the entire sheet is not known: The microwave interpolation field [see (*29*)] depends on factors other than accumulation (e.g., temperature) that may bias the outcome. There is also the difficulty that, although accumulation is averaged over decades or centuries, the ice-flux measurements are limited to those of the satellite measurements [1995 to 2000 in (*9*)]. This complicates comparison of the estimated mass imbalance with altimetry estimates whose interval [e.g., 1992 to 2003 in (*14*)] is precisely defined. To date, 58% of Antarctica has been surveyed, although the method may in principle be extended to the remainder. Some 70% of Greenland has also been surveyed, but the impact of the satellite observations in determining the time-averaged imbalance is lessened because runoff from land-terminated ice, which in Greenland accounts for some 60% of the mass loss, remains largely unmeasured. The range of estimates of net accumulation and runoff [169 to 283 Gt year^{-1} in (*1*), about 20% of the total accumulation] has complicated mass imbalance estimates for some time [e.g., (*30*, *31*)] and will continue to do so.

Satellite and aircraft, radar, and laser altimetry provide a detailed pattern of change in the ice sheets' interior (*7*, *10*, *14*, *17*, *18*) and have played a key role in distinguishing changes related to accumulation and ice dynamics. The longest records to date span 1992 to 2003 (*10*, *14*), and imbalances estimated from them differ from longer averages estimated by other methods as a result of fluctuations in accumulation and ablation. Ice cores [see (*7*)] and model reanalyses (*28*, *32*) show fluctuations in accumulation, relative to their temporal means, on the order of 15% in individual years, and a similar variability in rates of ablation (*32*, *33*) (Fig. 1). The problem is exacerbated because the density of snow differs from that of ice by a factor of three, and decadal fluctuations in snowfall mass are exaggerated in the observed volume fluctuations over those due to ice dynamics in the same ratio. A correction is possible if the snowfall fluctuation is independently known, but the only estimates available today are from meteorological forecast models, and a recent study (*14*) of Antarctica concluded that there was too little correspondence between the altimeter and meteorological data sets for this method to be reliable. Differences between estimates of mass change made from the same observations of volume change (*10*, *14*, *18*) arise largely through different approaches to the conversion of volume to mass. To give an idea of the uncertainty, Wingham *et al.* (*14*) showed that, in the absence of other data, an altimeter estimate covering 73% of the Antarctic interior could vary by 90 Gt year^{-1} without contradicting the observed volume change. ERS-1 and -2 radar altimetry (for which the longest records are available) has been limited to latitudes between 81.5°N and 81.5°S and to terrain of low slope. Because these regions lie in the ice sheet's interior, which is characterized by growth in Greenland in general and in Antarctica in some places, there is a tendency for these estimates to be more positive (Table 1). These difficulties may be overcome with the satellite laser altimeter records initiated by ICESat (Ice, Cloud, and land Elevation Satellite) in 2003 or, in the future, with the high-resolution radar altimeter of CryoSat-2.

Although differences in the time-averaged imbalances from the interferometric and altimetry methods are to be expected, the methods are highly complementary. For example, the retreat of the West Antarctic Pine Island Glacier grounding line observed by InSAR (*34*) is in close agreement with the drawdown of the inland ice observed with satellite altimetry (*23*). More recently, a combination of the two methods has provided considerable insight into the unstable hydraulic connection between subglacial lakes in East Antarctica (*35*).

The GRACE (Gravity Recovery and Climate Experiment) satellites have permitted the changing gravitational attraction of the ice sheets to be estimated (*11*, *13*, *15*, *16*, *19*, *20*). These estimates (Table 1) are more negative than those provided by mass budget or altimetry, but care is needed in making comparisons. The method is new, and a consensus about the measurement errors has yet to emerge [e.g., (*36*)], the correction for postglacial rebound is uncertain [e.g., (*37*)], contamination from ocean and atmosphere mass changes is possible [e.g., (*16*)], and the results depend on the method used to reduce the data [compare, e.g., (*20*) and (*16*)]. The GRACE record is also short (3 years) and, as was the case with early altimeter time series [e.g., (*7*)], is particularly sensitive to the fluctuations in accumulation described above. For example, whereas (*13*) puts the total 2002 to 2005 Antarctic Ice Sheet mass loss at 417 ± 219 Gt, a subsequent meteorological study (*38*) has put the 2002 to 2003 snowfall deficit at 309 Gt, a value that explains most of the observed change.

East Antarctica

Although the East Antarctic Ice Sheet (EAIS) is the largest reservoir of ice on Earth, it exhibits the smallest range of variability among recent mass balance estimates (Table 1). Since 1992, altimetric (*7*, *10*, *14*, *17*, *18*), interferometric (*9*), and gravimetric (*13*, *19*) surveys have put the EAIS annual mass trend in the range –1 to 67 Gt year^{-1}. Growth of the EAIS mitigates the current sea-level rise. Gains are limited to Dronning Maud Land and

Table 1. Mass balance (MB) of the East Antarctic (EAIS), West Antarctic (WAIS), Antarctic (AIS), and Greenland (GIS) ice sheets as determined by a range of techniques and studies. Not all studies surveyed all of the ice sheets, and the surveys were conducted over different periods within the time frame 1992 to 2006. For comparison, 360 Gt of ice is equivalent to 1 mm of eustatic sea-level rise.

Study	Survey period	Survey area 10^6 km^2 (%)	EAIS MB Gt year^{-1}	WAIS MB Gt year^{-1}	AIS MB Gt year^{-1}	GIS MB Gt year^{-1}
Wingham *et al.* (*7*)*	1992–1996	7.6 (54)	–1 ± 53	–59 ± 50	–60 ± 76	
Krabill *et al.* (*8*)*	1993–1999	1.7 (12)				–47
Rignot and Thomas (*9*)†	1995–2000	7.2 (51)	22 ± 23	–48 ± 14	–26 ± 37	
Davis and Li (*17*)*	1992–2002	8.5 (60)			42 ± 23	
Davis *et al.* (*10*)*	1992–2003	7.1 (50)	45 ± 7			
Velicogna and Wahr (*11*)‡	2002–2004	1.7 (12)				–75 ± 21
Zwally *et al.* (*18*)*	1992–2002	11.1 (77)	16 ± 11	–47 ± 4	–31 ± 12	11 ± 3
	1996					–83 ± 28
Rignot and Kanagaratnam (*12*)†	2000	1.2 (9)				–127 ± 28
	2005					–205 ± 38
Velicogna and Wahr (*20*)‡	2002–2005	12.4 (88)	0 ± 51	–136 ± 19	–139 ± 73	
Ramillien *et al.* (*19*)‡	2002–2005	14.1 (100)	67 ± 28	–107 ± 23	–129 ± 15	–169 ± 66
Wingham *et al.* (*14*)*	1992–2003	8.5 (60)			27 ± 29	
Velicogna and Wahr (*13*)‡	2002–2006	1.7 (12)				–227 ± 33
Chen *et al.* (*15*)‡	2002–2005	1.7 (12)				–219 ± 21
Luthcke *et al.* (*16*)‡	2003–2005	1.7 (12)				–101 ± 16
Range			–1 to 67	–136 to –47	–139 to 42	–227 to 11

*Altimetry. †InSAR mass budget. ‡Gravimetry.

Wilkes Land, and their spatial distribution (Fig. 2A) is strongly suggestive of snowfall-driven growth. Two glaciers in East Antarctica are losing mass (Fig. 2B). From 1992 to 2003, the fast-flowing trunks of the Totten and Cook glaciers deflated by 5.0 ± 0.5 and 2.4 ± 0.2 km^3 year^{-1}. Although these figures are only in rough coincidence with those determined from interferometry [0 ± 2 and -8 ± 5 km^3 year^{-1}, respectively, in (*9*)], the signals are clear and the trends definitely established.

West Antarctica and the Antarctic Peninsula

The West Antarctic Ice Sheet (WAIS) contains enough ice to raise global sea levels by more than 5 m and, according to altimetry and interferometry, one key sector is in a state of rapid retreat (*23*, *34*). Glaciers draining into the Amundsen Sea (Fig. 2A) are losing mass because of an ice-dynamic perturbation. During the 1990s, for example, the Pine Island Glacier retreated by up to 1.2 km year^{-1} (*34*), thinned by up to 1.6 m year^{-1} (*23*), and accelerated by around 10% (*39*); the ice loss has been implicated in the freshening of the Ross Sea some 1000 km away (*40*). Throughout the 1990s, independent altimeter (*7*, *14*, *17*, *18*) and interferometer (*9*) surveys of the WAIS as a whole were in notable, possibly fortuitous, agreement (Table 1), placing its annual losses in the range 47 to 59 Gt year^{-1}. The mass balance of the WAIS has been dominated by the losses from glaciers of the Amundsen sector, canceled to a degree by some snowfall-driven coastal growth and growth arising from the well-established shutdown of the Kamb Ice Stream (*41*).

There has been a report of an accelerated recent sea-level contribution (*42*) based on satellite and aircraft altimetry, and the gravimetric surveys have also estimated a rate of mass loss since 2002 of between 107 and 136 Gt year^{-1} (Table 1). Such an acceleration (an increase in sea-level trend of 0.2 mm year^{-1}, or about 10%) would be a cause for considerable concern. However, the altimeter data from which accelerated mass losses were derived in (*42*) span less than 5% of the WAIS area and use three altimeters with markedly different measurement errors. Furthermore, both data sets span a short time interval in which forecast models indicate that a 309-Gt accumulation deficit occurred (*38*). Taking these factors into account, it is unlikely that the WAIS mass loss has altered substantially since the 1990s.

During the past decade, there have been notable glaciological changes at the Antarctic Peninsula (AP): The Larsen Ice Shelf thinned (*43*) and sections collapsed (*44*), accelerating ice discharge into the oceans by some 0.07 mm year^{-1} ESL rise (*45*). However, the majority of AP ice forms the continental ice cap of Dyer Plateau. This exhibits snowfall-driven growth (Fig. 2A) that is sufficient to cancel the accelerated flow from the Larsen-A and -B catchments. The AP contribution to sea level is negligible.

Greenland

Since the most recent IPCC report, there have been seven estimates of Greenland mass imbalance based on satellite altimetry (*18*), interferometry (*12*), and gravimetry (*11*, *15*, *16*, *19*, *20*). There is consensus that during the 1990s the interior underwent modest snowfall-driven growth, which appears to be associated with a precipitation trend present in the meteorological record (*32*), offset by losses from lower altitude regions (Fig. 3, A and B). The decadal imbalance is not accurately determined. The more positive satellite altimeter estimate (*18*) is affected by signal loss in the steeper coastal margins; the aircraft laser measurements (*8*) are relatively sparse, although more sensitive to losses from marginal glaciers; and the mass-budget estimate (*12*) is undermined by the uncertainty of some 50 Gt year^{-1} in the accumulation. Nonetheless, the consensus of these measurements suggests a net loss in the 1990s of some 50 Gt year^{-1}.

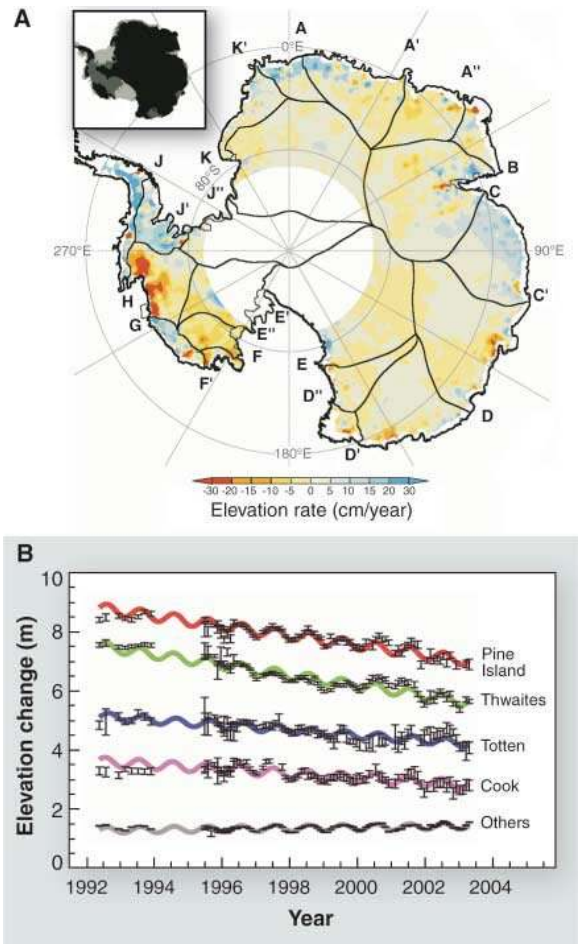

Fig. 2. (**A**) Rate of elevation change of the Antarctic Ice Sheet, 1992 to 2003, from ERS satellite radar altimetry [redrawn from (*14*)]. Also shown (inset) is the bedrock geometry, highlighting floating (light gray), marine-based (mid-gray) and continental-based (black) sectors. (**B**) Elevation change of the trunks (flow in excess of 50 m year^{-1}) of the Pine Island [Basin GH in (A)], Thwaites (Basin GH), Totten (Basin C′D), and Cook (Basin DD′) glaciers. All the deflating glaciers coincide with marine-based sectors of the ice sheet. An ice-dynamic origin of the thinning of the East Antarctic glaciers has yet to be confirmed by interferometry. However, the correlation of the thinning with flow velocity and the fact that the thinning rate is secular make ice dynamics the likely cause of all Antarctic mass losses.

Satellite interferometry (*12*, *24*) has also established that from 1996 to 2005, mass losses through flow increased by 102 Gt year^{-1}, and meteorological estimates (*32*) (Fig. 1B) of the surface-mass imbalance decreased some 20 Gt year^{-1} in the same period because of increased melting. Gravimetric surveys too support an increased mass loss (*11*, *15*, *16*, *19*, *20*). However, the interferometric and gravimetric records are short and reflect the considerable variability in the mass flux of tidewater glaciers and the surface mass balance. For example, the ice fluxes of two glaciers that by 2005 were responsible for 43 Gt year^{-1} of the increased discharge had by late 2006 declined to within 10 Gt year^{-1} of their level in 2000 (*46*), whereas in the past 14 years, the 3-year variability in surface mass imbalance has ranged from –130 to 120 Gt year^{-1} (Fig. 1B). In addition, not all gravimetric estimates capture the known spatial distribution of change; one that does (*16*) (Fig. 3B) is some 120 Gt year^{-1} more positive than other estimates, and some understanding of the cause of these discrepancies is needed. Increased mass loss from Greenland has occurred, but the decadal change is probably modest.

Implications for the Future

It is reasonable to conclude that, today, the EAIS is gaining some 25 Gt year^{-1}, the WAIS is losing about 50 Gt year^{-1}, and the GIS is losing about 100 Gt year^{-1}. These trends provide a sea-level contribution of about 0.35 mm year^{-1}, a modest component of the present rate of sea-level rise of 3.0 mm year^{-1}. Because 50 Gt year^{-1} is a very recent contribution, the ice sheets made little contribution to 20th-century sea-level rise. However, what has also emerged is that the losses are dominated by ice dynamics. Whereas past assessments (*47*) considered the balance between accumulation and ablation, the satellite observations reveal that glacier accelerations of 20 to 100% have occurred over the past decade. The key question today is whether these accelerations may be sustained, or even increase, in the future.

The question is difficult because the causes of the instabilities have yet to be established. The geo-

logical record (*48*) suggests that some 10,000 years ago, the Amundsen sector of the WAIS extended only 100 km farther than today, confining the present rate of retreat to more recent times, and the drawdown of the Amundsen sector ice streams has been linked (*49*) to a recent trigger in the ocean. A comparable argument may be extended to the thinning glaciers in East Antarctica and Greenland, which are also marine terminated. Equally, there is no direct evidence of a warming of the Amundsen Sea, and it has long been held possible that the marine-terminated WAIS, and the Amundsen sector in particular, may be geometrically unstable (*50*), and the retreating East Antarctica streams have a similar geometry (Fig. 2A). In Greenland, where summer melting is widespread and increasing, Global Positioning System measurements have shown the melting to affect flow velocity in the ice sheet interior (*26*), introducing the possibility that increased surface meltwater is reaching the bed and accelerating the ice flow to the ocean.

The discovery that particular ice streams and glaciers are dominating ice sheet mass losses means that today our ability to predict future changes is limited. Present numerical models capture neither the details of actual ice streams nor, in Greenland, those of hydraulic connections between the surface and the bed. In addition, the detailed mechanics at the grounding line still remain to be fully worked out. In consequence, the view that the changing sea-level contribution of the Antarctic and Greenland ice sheets in the 21st century will be both small and negative as a result of accumulating snow in Antarctica [e.g., –0.05 mm year^{-1} in (*1*)] is now uncertain.

Because our predictive ability is limited, continued observation is essential. The satellite record clearly identifies the particular ice streams and glaciers whose evolution is of greatest concern. The causes of their instability need to be identified. Their detailed basal topography, their basal hydrology, and the details of the interaction with their surrounding shelf seas need to be established. Numerical models that capture the detailed dynamics of these glaciers and their hydrology are required. Of equal importance are meteorological and ice core measurements that will increase confidence in forecast models of accumulation and ablation fluctuations, because to a considerable extent these limit interpretations of the short satellite records. There is a great deal that the International Polar Year may achieve.

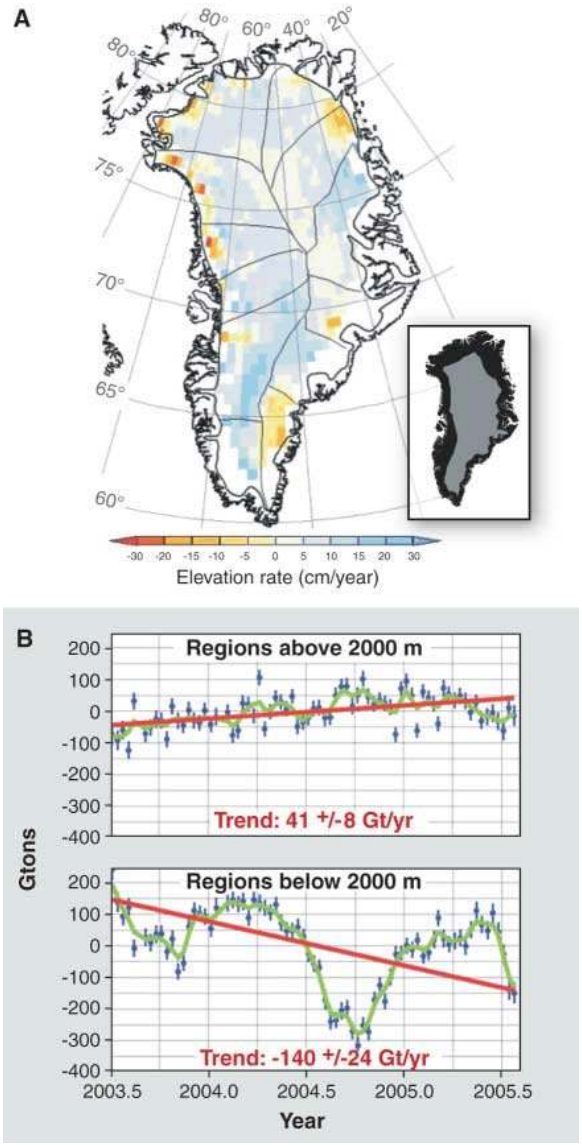

Fig. 3. (**A**) Rate of elevation change of the Greenland Ice Sheet, 1992 to 2003, determined from satellite radar altimetry [from (*22*)], and (**B**) time series of elevation change of individual sectors, 2003 to 2005, determined from satellite gravimetry [from (*16*)]. Also shown (inset) is the ice surface geometry, highlighting areas above (gray) and below (black) 2000 m elevation. Both instruments concur that high elevation areas are growing and low elevation areas are losing mass. According to gravimetry (*16*) and repeat InSAR measurements of ice discharge (*12*), the rate of mass loss at low elevations has increased over the past decade (see Table 1).

References and Notes

1. J. A. Church, J. M. Gregory, in *Climate Change 2001: The Scientific Basis*, J. T. Houghton *et al.*, Eds. (Cambridge Univ. Press, Cambridge, 2001), chap. 11, pp. 641–693.
2. R. G. Fairbanks, *Nature* **342**, 637 (1989).
3. N. Stern, *The Economics of Climate Change: The Stern Review* (Cambridge Univ. Press, Cambridge, 2006).
4. C. S. Benson, "Stratigraphic studies in the snow and firn of Greenland ice sheet" Research Report 70 (Cold Regions Research and Engineering Lab, Hanover, NH, 1962).
5. C. R. Bentley, M. B. Giovinetto, Proceedings of the International Conference on the Role of Polar Regions in Global Change (Geophysical Institute, University of Alaska, Fairbanks, AK, 1991), pp. 481–486.
6. S. S. Jacobs, *Nature* **360**, 29 (1992).
7. D. J. Wingham, A. Ridout, R. Scharroo, R. Arthern, C. K. Shum, *Science* **282**, 456 (1998).
8. W. Krabill *et al.*, *Science* **289**, 428 (2000).
9. E. Rignot, R. H. Thomas, *Science* **297**, 1502 (2002).
10. C. H. Davis, Y. Li, J. R. McConnell, M. M. Frey, E. Hanna, *Science* **308**, 1898 (2005).
11. I. Velicogna, J. Wahr, *Geophys. Res. Lett.* **32**, art-L18505 (2005).
12. E. Rignot, P. Kanagaratnam, *Science* **311**, 986 (2006).
13. I. Velicogna, J. Wahr, *Science* **311**, 1754 (2006).
14. D. J. Wingham, A. Shepherd, A. Muir, G. J. Marshall, *Philos. Trans. R. Soc. A Math. Phys. Eng. Sci.* **364**, 1627 (2006).
15. J. L. Chen, C. R. Wilson, B. D. Tapley, *Science* **313**, 1958 (2006).
16. S. B. Luthcke *et al.*, *Science* **314**, 1286 (2006).
17. C. H. Davis, Y. H. Li, paper presented at Science for Society: Exploring and Managing a Changing Planet (IEEE, Anchorage, Alaska, 20–24 Sep 2004), pp. 1152–1155.
18. H. J. Zwally *et al.*, *J. Glaciol.* **51**, 509 (2005).
19. G. Ramillien *et al.*, *Global Planet. Change* **53**, 198 (2006).
20. I. Velicogna, J. Wahr, *Nature* **443**, 329 (2006).
21. W. Munk, *Science* **300**, 2041 (2003).
22. O. M. Johannessen, K. Khvorostovsky, L. P. Bobylev, *Science* **310**, 1013 (2005).
23. A. Shepherd, D. J. Wingham, J. A. D. Mansley, H. F. J. Corr, *Science* **291**, 862 (2001).
24. I. Joughin, W. Abdalati, M. Fahnestock, *Nature* **432**, 608 (2004).
25. A. Luckman, T. Murray, R. de Lange, E. Hanna, *Geophys. Res. Lett.* **33**, art-L03503 (2006).
26. H. J. Zwally *et al.*, *Science* **297**, 218 (2002).
27. R. Bindschadler, *Science* **311**, 1720 (2006).
28. A. J. Monaghan, D. H. Bromwich, S. H. Wang, *Philos. Trans. R. Soc. A Math. Phys. Eng. Sci.* **364**, 1683 (2006).
29. R. J. Arthern, D. P. Winebrenner, D. G. Vaughan, *J. Geophys. Res. Atmos.* **111**, D06107 (2006).
30. E. J. Rignot, S. P. Gogineni, W. B. Krabill, S. Ekholm, *Science* **276**, 934 (1997).
31. N. Reeh, H. H. Thomsen, O. B. Olesen, W. Starzer, *Science* **278**, 205 (1997).
32. J. E. Box *et al.*, *J. Clim.* **19**, 2783 (2006).
33. N. P. M. van Lipzig, E. van Meijgaard, J. Oerlemans, *Int. J. Climatol.* **22**, 1197 (2002).
34. E. J. Rignot, *Science* **281**, 549 (1998).
35. D. J. Wingham, M. J. Siegert, A. Shepherd, A. S. Muir, *Nature* **440**, 1033 (2006).
36. M. Horwath, R. Dietrich, *Geophys. Res. Lett.* **33**, art-L07502 (2005).
37. M. Nakada *et al.*, *Mar. Geol.* **167**, 85 (2000).
38. A. J. Monaghan *et al.*, *Science* **313**, 827 (2006).
39. I. Joughin, E. Rignot, C. E. Rosanova, B. K. Lucchitta, J. Bohlander, *Geophys. Res. Lett.* **30**, 1706 (2003).
40. S. S. Jacobs, C. F. Giulivi, P. A. Mele, *Science* **297**, 386 (2002).
41. S. Anandakrishnan, R. B. Alley, *Geophys. Res. Lett.* **24**, 265 (1997).
42. R. Thomas *et al.*, *Science* **306**, 255 (2004).
43. A. Shepherd, D. Wingham, T. Payne, P. Skvarca, *Science* **302**, 856 (2003).
44. H. Rott, P. Skvarca, T. Nagler, *Science* **271**, 788 (1996).
45. E. Rignot *et al.*, *Geophys. Res. Lett.* **31**, art-L18401 (2004).
46. I. M. Howat, I. Joughin, T. A. Scambos, *Science* **315**, 1559 (2007).
47. R. B. Alley, P. U. Clark, P. Huybrechts, I. Joughin, *Science* **310**, 456 (2005).
48. A. L. Lowe, J. B. Anderson, *Quat. Sci. Rev.* **21**, 1879 (2002).
49. A. J. Payne, A. Vieli, A. P. Shepherd, D. J. Wingham, E. Rignot, *Geophys. Res. Lett.* **31**, art-L23401 (2004).
50. J. Weertman, *J. Glaciol.* **13**, 3 (1974).

10.1126/science.1136776

Rapid Changes in Ice Discharge from Greenland Outlet Glaciers

Ian M. Howat,[1,2]* Ian Joughin,[1] Ted A. Scambos[2]

Using satellite-derived surface elevation and velocity data, we found major short-term variations in recent ice discharge and mass loss at two of Greenland's largest outlet glaciers. Their combined rate of mass loss doubled in less than a year in 2004 and then decreased in 2006 to near the previous rates, likely as a result of fast re-equilibration of calving-front geometry after retreat. Total mass loss is a fraction of concurrent gravity-derived estimates, pointing to an alternative source of loss and the need for high-resolution observations of outlet dynamics and glacier geometry for sea-level rise predictions.

The recent, marked increase in ice discharge from many of Greenland's large outlet glaciers has upended the conventional view that variations in ice-sheet mass balance are dominated on short time scales by variations in surface balance, rather than ice dynamics. Beginning in the late 1990s and continuing through the past several years, the ice-flow speed of many tidewater outlet glaciers south of 72° North increased by up to 100%, increasing the ice sheet's contribution to sea-level rise by more than 0.25 mm/year (*1*). The synchronous and multiregional scale of this change and the recent increase in Arctic air and ocean temperatures suggest that these changes are linked to climate warming. The possibility that ice dynamics are so highly sensitive to climate change is of concern, because the physical processes that would drive such a relationship are poorly understood and are not realistically included in ice-sheet models used to predict rates of sea-level rise.

Current estimates of change in Greenland's ice discharge are based on velocity measurements taken 4 to 5 years apart (*1*). However, 50 to 100% increases in ice speed and thinning of tens of meters over a single year have been documented in Greenland and elsewhere (*2*–*6*). Therefore, discharge should be highly variable as well, even at subannual time scales. Large increases in tidewater glacier speed have been attributed to decreased flow resistance and increased along-flow stresses during retreat of the ice front (*2*, *3*, *7*). This suggests that changes in velocity and discharge are coupled to changes in tidewater glacier geometry and that the observed rapid changes may be a transient response to disequilibrium at the front. Therefore, accurate estimates of current rates of discharge and the potential for near-future change require observations of outlet glacier geometry and speed at high temporal resolution.

To assess short-term variability in outlet glacier dynamics, we examined speed, geometry, and discharge at two of Greenland's three largest outlet glaciers between 2000 and 2006. Located on the central east coast, Kangerdlugssuaq (KL) and Helheim (HH) represent 35% of east Greenland's total discharge (*1*). The calving fronts of both glaciers appeared relatively stable from the mid-20th century (*8*, *9*) until 2002, when HH retreated more than 7 km in 3 years (*2*). This was followed by a 5-km retreat of KL during the winter of 2004 to 2005 (*4*). These retreats are much greater than the 1- to 2-km seasonal fluctuations previously observed (*4*, *5*) and followed a sustained period of low-elevation ice thinning (*8*, *10*). Retreats were concurrent with accelerated ice flow (*1*, *2*). This acceleration increased rates of mass loss by 28 and 15 Gt/year at KL and HH, respectively, between 2000 and 2005, representing >40% of the ice sheet's increase in mass loss (*1*).

We measured summer surface speed and elevation for these glaciers using imagery acquired by the Advanced Spaceborne Thermal Emission and Reflection radiometer (ASTER) sensor aboard the Terra satellite, launched in 1999. We constructed Photogrammetric Digital Elevation Models (DEMs) from ASTER stereobands (3N and 3B) and validated them (Figs. 1D and 2D) using laser altimetry data sets collected by NASA's Airborne Topographic Mapper (ATM) in 2001, 2003, and 2005 (*10*). The root-mean-squared differences between DEM and ATM elevations are 10 m, which is similar to the uncertainty quoted in ASTER DEM validation studies (*11*) (Figs. 1D and 2D). Summer surface velocity was obtained from automated feature tracking between repeat, orthorectified principal component images of bands 1 to 3 (*2*, *12*). Uncertainty in these measurements is ~5 m per image pair, or 0.1 to 0.8 m/day for the data presented here. We determined winter velocities (±3% uncertainty) using radar speckle tracking between Canadian Space Agency Radar Satellite

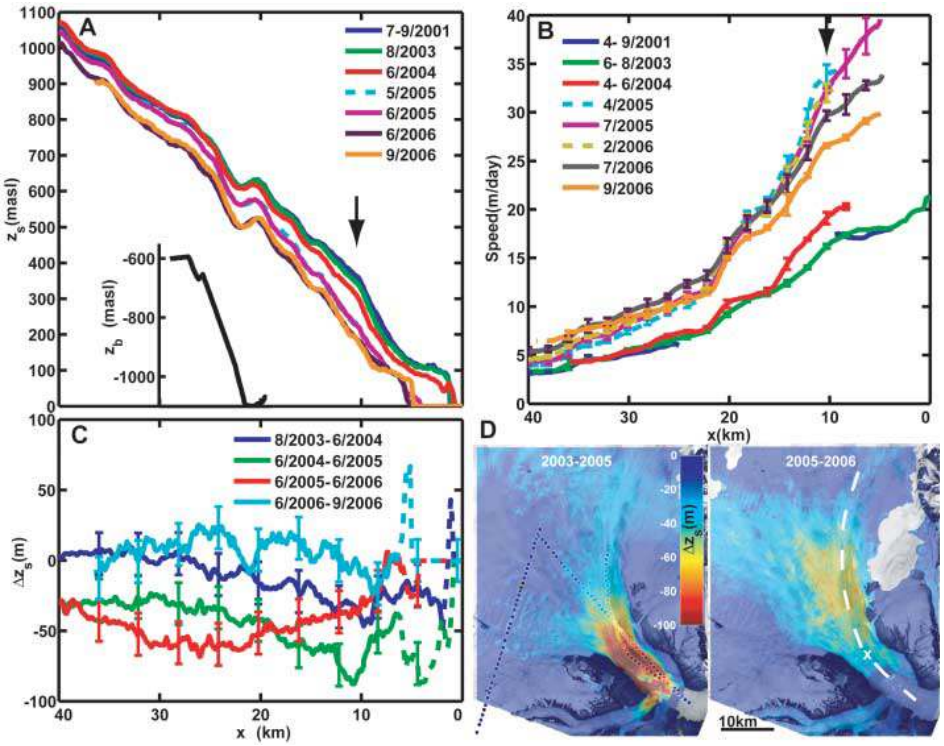

Fig. 1. KL glacier. (**A**) Surface elevation (z_s) from (solid) ASTER DEMs and (dashed) Airborne ATM laser altimetry and bed elevation (z_b) from CoRDS. (**B**) Surface velocity obtained from (solid) optical feature tracking and (dashed) radar speckle tracking along the main flow line, denoted by white dashes in (D). Arrows point to location of flux gate used for discharge calculation. (**C**) Elevation change along the same profile. Dashed segments are changes due to movement of the ice front. (**D**) Maps of elevation change from differenced ASTER DEMs overlaid on the 21 June 2005 image. Circles show repeat ATM altimetry measurements for the same time period and x marks flux-gate location. Error bars in (B) and (C) show means ± SD.

[1]Polar Science Center, Applied Physics Lab, University of Washington, 1013 Northeast 40th Street, Seattle, WA 98105–6698, USA. [2]National Snow and Ice Data Center, University of Colorado, 1540 30th Street, Boulder, CO, 80309–0449, USA.

*To whom correspondence should be addressed. E-mail: ihowat@apl.washington.edu

(RADARSAT) image pairs (24-day separation) (*13*). In some cases, combinations of multiple elevation and speed data sets from the same season improved spatial coverage and reduced errors. The University of Kansas Coherent Radar Depth Sounder (CoRDS) surveyed ice thickness and bed elevation at both glaciers in 2001 (*14*).

From summer 2004 to spring 2005, KL retreated by 5 km (*4*), and its speed increased by 80% near the front and by ~20% at 30 km inland (Fig. 1). Between April and July 2005, the increase in speed migrated rapidly inland with a ~5% decrease in speed close to the front and a ~7% increase in speed in areas farther inland (up-glacier). This upstream propagation continued from July 2005 through July 2006, with the near-front deceleration of ~15% and up-glacier acceleration of ~25%, with the transition between speedup and slowdown at ~15 km. The glacier thinned rapidly during acceleration, with 80 m of thinning near the front and thinning of at least 40 m extending 40 km inland by summer 2005. Thinning moved inland between 2005 and 2006, with a peak thinning of 68 m at about 26 km, but with virtually no thinning at the front. Average thinning over the glacier during the summer of 2006 declined to near zero, with some apparent thickening in areas on the main trunk.

Images from June 2003 are the first to indicate substantial retreat (2.1 km) at HH. During additional retreat over that summer, speedup of 20 to 40% extended at least 20 km up-glacier (Fig. 2). The ice front and speed changed little in 2004, but 4 km of new retreat yielded another major speedup (25%) in the summer of 2005. Many of the earlier data do not extend far inland, but echoing the pattern on KL, speeds from 2006 show a progressive inland acceleration accompanied by deceleration (25%) extending from about 15 km toward the ice front. As with KL, rapid thinning accompanied the large speed increases. By late summer 2006, strain rates indicate a region of compression at about 12 to 15 km. The initial HH acceleration in 2003 produced 40 m of thinning within about 15 km of the ice front. This thinning slowed to 10 m/year when there was little retreat from 2003 to 2004. The 4-km retreat from 2004 to 2005 moved the ice front over a 200-m bathymetric depression, bringing it to or near flotation. Between the summers of 2005 and 2006, the rate of thinning decreased within 20 km of the front, reaching zero at the front and increasing to 50 m/year 25 km from the front. During this period, the glacier advanced 4 km as a floating or near-floating tongue to near the 2003–2004 front position. It appears that the front of this floating tongue may have regrounded in summer 2006, contributing to the deceleration and the region of compression.

On both KL and HH, the data show a markedly similar progression of increasing down-glacier speed and thinning synchronous with retreat, followed by an inland migration of the speed increase. As the front restabilized, speed and thinning increased up-glacier and decreased down-glacier. This progression of dynamic response strongly suggests that the notable increases in acceleration and thinning are related to changes in calving-front position through variations in longitudinal stresses (*2*). Consistent with standard theories of tidewater glacier dynamics (*15*), rapid retreat at HH occurred as the front moved into deeper water and stopped where the bed slope reversed (Fig. 2). At both glaciers, the initial acceleration and thinning after retreat were concentrated within 10 to 20 km of the ice front, which would be the expected range of stress coupling (*16*). Relative thinning down-glacier increases the surface slope and driving stress up-glacier. By this means, thinning and acceleration are advected up-glacier (*17*). This can be seen at KL, where the maximum thinning rates moved ~10 km up-glacier between 2005 and 2006 (Fig. 1). This propagation rate is equal to about five times the distance-integrated 2005 ice speed, which is the approximate rate of advection of a kinematic wave traveling through ice (*18*).

We estimated discharge anomalies relative to the year 2000, when the glaciers were near balance, taking into account the changes in both speed and thickness (Fig. 3). At each glacier, our discharge estimates from 2000 to 2005 agree closely with mass-budget estimates (*1*). At KL, roughly 80% of the total increase in discharge occurred in less than 1 year in 2005, followed by a 25% drop the next year (Fig. 3). At HH, discharge increased 5 Gt/year between 2000 and

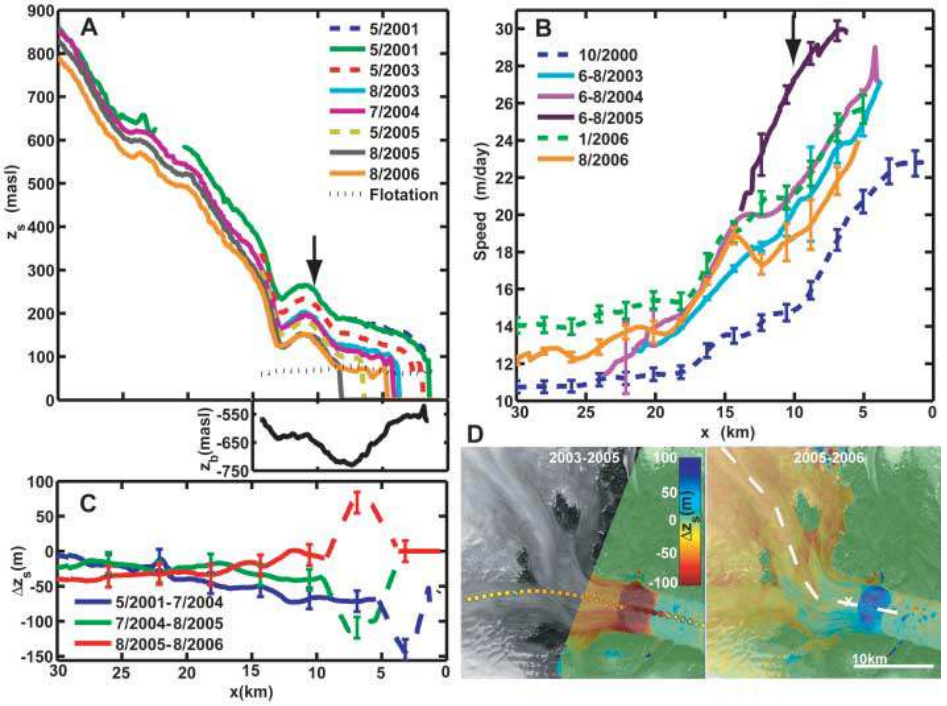

Fig. 2. (**A** to **D**) Same as Fig. 1 for HH, except (D) uses a 29 August 2005 image background.

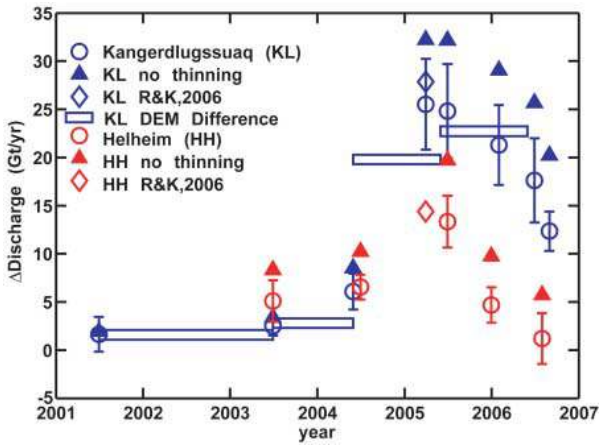

Fig. 3. Discharge anomaly from year 2000. Circles with error bars are calculated from speed and thickness change across flux gates shown in Figs. 1 and 2 with initial ice thickness obtained by dividing the year 2000 flux by the product of glacier width and 2000 speed (*1*). Uncertainties are the combinations of errors in ice elevation and speed. Triangles are the discharge anomaly with ice thickness held constant. Diamonds are the 2000 to 2005 discharge-change values from mass budget (*1*). Rectangles are KL mass-loss estimates from differencing repeat on-ice ASTER DEMs over the area shown in Fig. 1D. Spatial DEM coverage for HH is incomplete, preventing mass-loss calculations. The horizontal ranges in these estimates are the image acquisition dates, and the vertical range is the uncertainty.

2003 and by another 7 Gt/year between 2004 and 2005. It then dropped by more than 13 Gt/year in 2006, returning to near its 2000 value.

Integrating the time series of discharge anomaly from 2000 to 2006 gives totals of 52 Gt at KL and 30 Gt of excess discharge at HH (Fig. 3). Extensive DEM coverage of KL allows for a direct estimate of volume change over the lower basin (47 Gt), excluding any additional thinning at higher elevation. This loss estimate (47 Gt) agrees well with the KL discharge anomaly. When the existing imbalances from 2000 are factored in, the combined net loss of ice from 2000 to 2006 is 90 Gt, with 63 Gt of this loss in the interval from summer 2004 to summer 2006. The sharp increase in mass loss through these glaciers between 2004 and 2005 (32 Gt) can explain about 30% of the mass loss indicated by Gravity Recovery and Climate Experiment (GRACE) gravity observations for southeast Greenland (*19*).

Other GRACE observations suggest a 450 Gt ice loss from south Greenland between May 2004 and April 2006 that the authors mostly attribute to increased discharge from HH and KL (*20*). Although the timing of the increased loss agrees well with the KL and HH acceleration, our results suggest that the combined loss from these glaciers over this period can only account for 13% of this loss. Absent an extensive but unobserved acceleration elsewhere, measurements for other south Greenland glaciers suggest a loss increase from 2000 to 2005 of roughly 23 Gt/year (*1*). This suggests that despite large dynamic changes, much of the loss between 2004 and 2006 estimated from GRACE may be related to surface balance anomalies or other causes.

Our results indicate that large variations in outlet glacier discharge can produce large discharge anomalies in a span of a few years. Although the initial triggering for the recent changes is unclear, it is well known that very small perturbations to thickness can induce retreat in calving glaciers (*15*). In the cases we examined, large imbalances appear to have caused rapid adjustments in the glacier geometry, leading to a quick (~2-year) return to near balance, though some degree of moderate thinning may persist. The surface drawdown of 100 m or more at low elevations within the outlets may have substantial effects on summertime surface melt rates, potentially predisposing them to further ice thinning and retreat. However, prediction of near-future change will require detailed data on bed elevation and ice thickness. This is not yet available for most of the outlet glaciers.

Dynamic re-equilibration after a perturbation in geometry may not always be as rapid as observed here. For example, Jakobshavn Isbrae has maintained high speeds for several years after retreat and acceleration (fig. S1) (*3*). In this case, retreat from the fjord increased inflow from the sides, potentially resulting in lower thinning rates (~15 m/year) (*5*, *10*). Likewise, many glaciers along Greenland's northwest coast have retreated into the ice sheet with sustained thinning at rates of a few meters per year but show no apparent change in speed (*1*). This suggests that geometry and other characteristics unique to each glacier may determine the time scale over which discharge anomalies occur.

The highly variable dynamics of outlet glaciers suggest that special care must be taken in how mass-balance estimates are evaluated, particularly when extrapolating into the future, because short-term spikes could yield erroneous long-term trends. Rather than yielding a well-defined trend, our results are notable in that they show that Greenland mass balance can fluctuate rapidly. If these changes are the result of recent warm summers (*21*), continued warming may cause a long-term drawdown of the ice sheet through a series of such discharge anomalies, perhaps with a similar degree of variability. Therefore, accurate estimates of ice-sheet mass balance will require subannual observations of outlet glacier dynamics to avoid aliasing this rapidly varying signal.

References and Notes

1. E. Rignot, P. Kanagaratnam, *Science* **311**, 986 (2006).
2. I. M. Howat, I. Joughin, S. Tulaczyk, P. Gogineni, *Geophys. Res. Lett.* **32**, L22502 (2005).
3. I. Joughin, W. Abdalati, M. Fahnestock, *Nature* **432**, 608 (2004).
4. A. Luckman, A. Murray, R. De Lange, E. Hanna, *Geophys. Res. Lett.* **33**, L03503 (2006).
5. R. H. Thomas *et al.*, *J. Glaciol.* **49**, 231 (2003).
6. T. A. Scambos, J. A. Bohlander, C. A. Shuman, P. Skvarca, *Geophys. Res. Lett.* **31**, L18402 (2004).
7. R. H. Thomas, *J. Glaciol.* **50**, 57 (2004).
8. R. H. Thomas *et al.*, *Geophys. Res. Lett.* **27**, 1291 (2000).
9. A. Weidick, *U.S. Geol. Surv. Prof. Pap. 386-C* (1995), pp. C85–C87.
10. W. Krabill *et al.*, *Geophys. Res. Lett.* **31**, L24402 (2004).
11. B. T. San, M. L. Suzen, *Int. J. Remote Sens.* **26**, 5013 (2005).
12. T. A. Scambos, M. J. Dutkiewicz, J. C. Wilson, R. A. Bindschadler, *Remote Sens. Environ.* **42**, 177 (1992).
13. I. Joughin, *Ann. Glaciol.* **34**, 195 (2002).
14. S. Gogineni *et al.*, *J. Geophys. Res.* **106**, 33761 (2001).
15. M. F. Meier, A. Post, *J. Geophys. Res.* **92**, 9051 (1987).
16. B. Kamb, K. A. Echelmeyer, *J. Glaciol.* **32**, 267 (1986).
17. A. J. Payne, A. Vieli, A. P. Shepherd, D. J. Wingham, E. Rignot, *Geophys. Res. Lett.* **31**, L23401 (2004).
18. C. J. Van der Veen, in *Fundamentals of Glacier Dynamics* (A. A. Balkema, Rotterdam, Netherlands, 1999), p. 313.
19. S. B. Luthcke *et al.*, *Science* **314**, 1286 (2006).
20. I. Velicogna, J. Wahr, *Nature* **443**, 329 (2006).
21. I. Joughin, *Science* **311**, 1719 (2006).

22. NASA grants NNG06GE5SG and NNG06GE50G supported the contribution of I.M.H. and T.A.S. NSF grant ARC-0531270 supported I.R.J.'s contribution.

Supporting Online Material

www.sciencemag.org/cgi/content/full/1138478/DC1
Fig. S1
Reference

6 December 2006; accepted 24 January 2007
Published online 8 February 2007;
10.1126/science.1138478
Include this information when citing this paper.

Conformationally Controlled Chemistry: Excited-State Dynamics Dictate Ground-State Reaction

Myung Hwa Kim,[1,2] Lei Shen,[1] Hongli Tao,[3] Todd J. Martinez,[3]* Arthur G. Suits[1,2]*

Ion imaging reveals distinct photodissociation dynamics for propanal cations initially prepared in either the cis or gauche conformation, even though these isomers differ only slightly in energy and face a small interconversion barrier. The product kinetic energy distributions for the hydrogen atom elimination channels are bimodal, and the two peaks are readily assigned to propanoyl cation or hydroxyallyl cation coproducts. Ab initio multiple spawning dynamical calculations suggest that distinct ultrafast dynamics in the excited state deposit each conformer in isolated regions of the ground-state potential energy surface, and, from these distinct regions, conformer interconversion does not effectively compete with dissociation.

From stereoselective synthesis to protein folding, conformational dynamics lie at the heart of chemistry (*1*). Molecular conformers typically interconvert via hindered rotations about single bonds, and the low energy barriers to these processes lead to equilibration even at low temperatures. Recent efforts to explore the detailed conformational energy landscapes of molecules have relied on stimulated emission pumping in jet-cooled beams, exciting then re-trapping molecules in different local minima to probe the interconversion barriers (*2*, *3*). Single-molecule methods have also been used to investigate conformational heterogeneity: Otherwise identical molecules exhibit vastly different rates in key steps of enzymatic processes (*4*, *5*). Conformational selectivity has been suggested as a means of achieving laser control of chemical outcomes (*6*). However, the low barriers for intercon-

[1]Department of Chemistry, Wayne State University, Detroit, MI 48202, USA. [2]Department of Chemistry, Stony Brook University, Stony Brook, NY 11794, USA. [3]Department of Chemistry, University of Illinois, Champaign, IL 61801, USA.

*To whom correspondence should be addressed. E-mail: asuits@chem.wayne.edu (A.G.S.); tjm@spawn.scs.uiuc.edu (T.J.M.)